

Performance Evaluation of Optical Subcarrier Multiplexed Systems using Transient Analysis

R Rajaduray* and D. J. Blumenthal†

Optical Communications and Photonic Networks, ECE Department, UCSB, Santa Barbara, CA
93107

ABSTRACT

Results are presented of an investigation into the performance of an optical subcarrier multiplexed (OSCM) system using a novel simulation approach. The OSCM system analyzed is based upon two systems which have been demonstrated experimentally previously. Intersymbol interference and crosstalk degradation effects for both the baseband and subcarrier signals are calculated

Keywords: Subcarrier multiplexing, intersymbol interference, crosstalk, optical filters, optical transfer functions, transient analysis, error analysis

1. INTRODUCTION

Optical subcarrier multiplexing (OSCM) wherein baseband (BB) signals are combined with microwave subcarrier (SC) signals, has been shown to be a valuable technique for the transmission of control information in optical networks [1] [2]. They have also been used for optical performance monitoring [3], [4] and all-optical label swapping. [5 - 7].

In this paper, the crosstalk performance of an OSCM channel, where the SC channel is used for control signaling while the BB channel is used for data is evaluated. This is done using a novel transient analysis approach incorporating the saddlepoint approximation. Previous approaches have used the steady-state power transfer functions to analyze the crosstalk performance.

This analysis concentrates on an architecture using a loop mirror filter (LMF). This architecture has been demonstrated in [8],[9] and [10] for the multiplexing and demultiplexing of OSCM signals respectively.

2. MOTIVATION

A network composed of OSCM routers is illustrated in Figure 1. The SC data is used for control signaling. This includes information for topology discovery, distributed routing, dynamic lightpath provisioning and traffic engineering. In the case of an MPLS network, it can be used to disseminate label distribution protocol information. Other methods such as out-of-band signaling can also be used to transmit control information.

In the OSCM router architecture of Figure 2, incoming combined BB and SC data is demultiplexed using the filter demonstrated in [8], [9]. The SC data is then processed, and relevant information is then sent to the control plane of the router, which could then use this information for regeneration and signal conditioning of the BB data, as well as QoS-capable IP forwarding and constraint-based routing. In this study it is assumed that the SC channel is continually active.

Crosstalk degradation arises because the response of the signals after multiplexing and demultiplexing takes time to settle to the steady-state response. This degradation is dependent on factors such as misalignment between the bit streams, the influence of the transient response of the filters and pattern-dependent effects in both the BB and SC bit streams.

* meshraj@engineering.ucsb.edu; phone 1 805 893 5282; fax 1 805 893 5705

† danb@ece.ucsb.edu; phone 1 805 893 4168; fax 1 805 893 5705

Previous approaches [11] – [13] have used the steady-state power transfer functions to analyze the degradation to the bit error rate due to crosstalk. This however does not fully reflect the transient nature of the factors mentioned above.

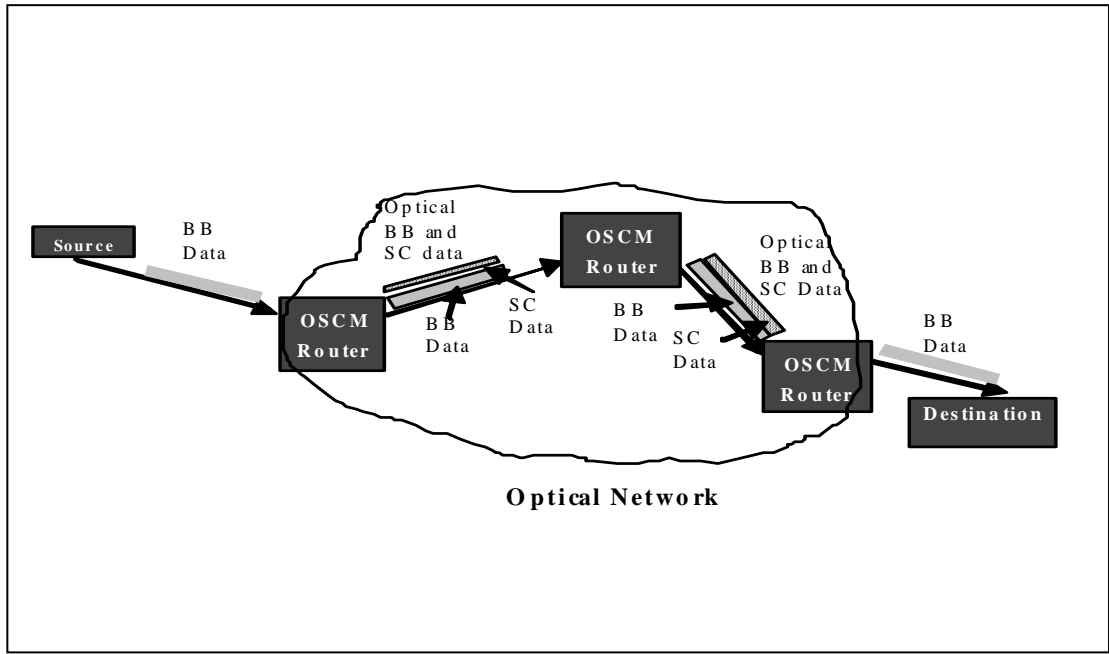


Figure 1: Example Network with OSCM Signaling

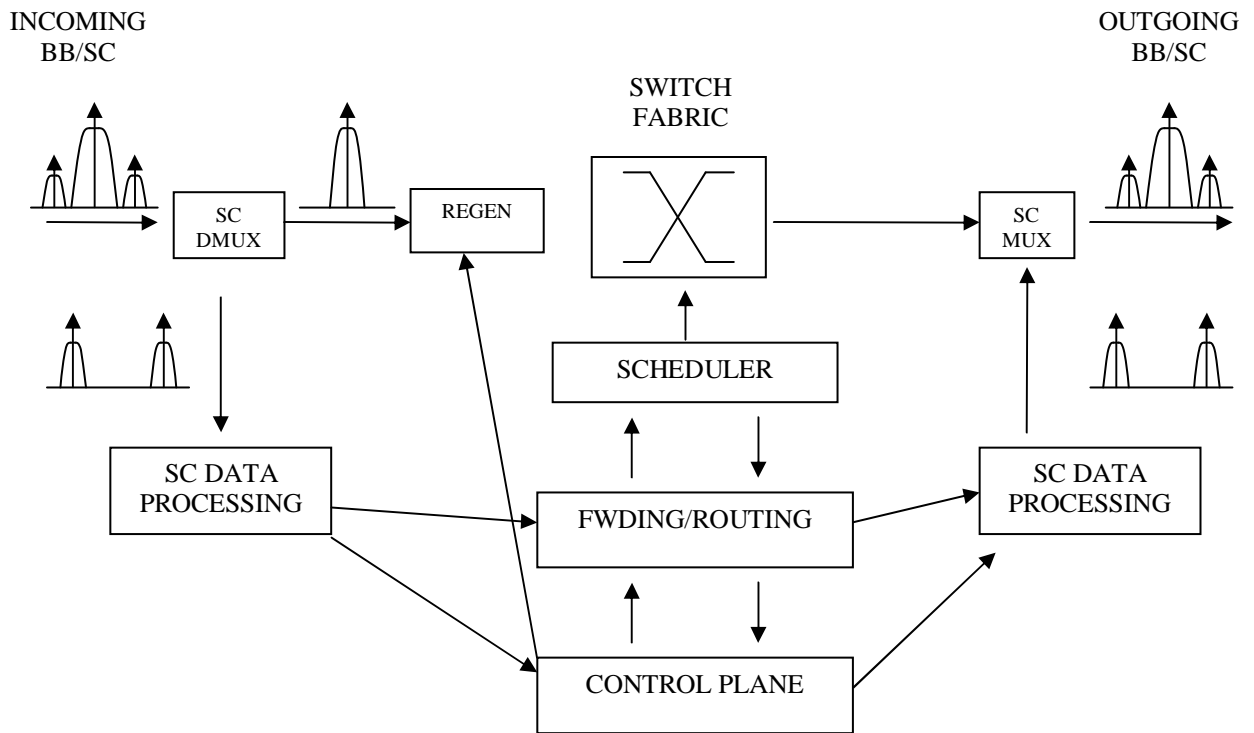


Figure 2: Example OSCM Router Architecture

Another method would be to use a Monte Carlo approach to evaluate the bit error rate. However, there are many difficulties involved in evaluating the extremely low bit error rates (for example 10^{-9} or lower) typically of interest in optical communications systems.

The analysis used in this paper fully captures the degradation due to these transient factors, and also the optical phase mismatch between the BB and SC. The saddlepoint approximation is used to calculate the bit error rates. This has been shown previously [14] – [16] to be a highly accurate method of evaluating bit error rates for systems with crosstalk degradation, and in [9] to evaluate the power penalty due to ISI after subcarrier prefiltering by a loop mirror filter (LMF). To our knowledge, this is the first time that such an approach has been used to calculate crosstalk degradation in an OSCM system.

3. NOVEL TRANSIENT APPROACH TO CROSSTALK DEGRADATION EVALUATION

Figure 3 is a reference model for the calculations carried out in this paper. It shows a digital optical data channel, with an interfering digital data optical crosstalk channel, passing through a subsystem designed to drop the data channel. This subsystem could be part of the front-end of one of the routers as shown in Figure 1.

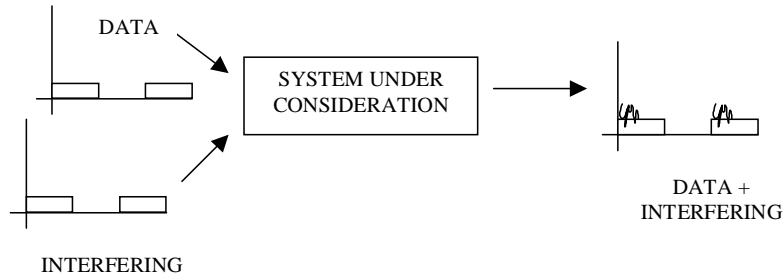


Figure 3: Crosstalk Reference Model

The data channel suffers crosstalk due to the interfering channel. First, consider only the data channel. The electrical field envelope $E(t)$ is given by the expression:

$$E(t) = A \cdot \sum_{k=-\infty}^{\infty} a_k h(t - kT_{b,BB}) \quad (1)$$

where A is the amplitude of the field. a_k can be either a '0' or a '1', and $h(t)$ is the normalized pulse shape used in the data channel. This signal is incident on the receiver of Figure 3. At the receiver the mean number of electrons $\lambda(t)$ generated at time t , is proportional to the power incident on the photodetector.

The power incident is dependent upon random variables $x_1, x_2 \dots x_n$ in the optical domain such as the pattern of past bits; optical amplifier noise; or electrical phase uncertainty in the case of an RF-modulated optical signal. Denoting the considered bit as a_0 , the power can then be conditioned upon values of these random variables. The mean number of electrons $\lambda(t)$ is then given by:

$$(\lambda(t)|_{a_0 = 0,1, x_1, x_2 \dots}) = \frac{\eta}{h\nu} |(E(t)|_{a_0, x_1, x_2 \dots})|^2 \quad (2)$$

where η is the quantum efficiency, and ν is the frequency of the optical carrier. $\lambda(t)$ is conditioned on $a_0 = 0$ and $a_0 = 1$, to obtain pdfs for a '0' or a '1' received. This result is then amplified by a current amplifier with gain G and integrated over an integration period T , to yield a total electron count Λ for the process, given by:

$$\left(\Lambda|a_0 = 0,1, x_1, x_2 \dots\right) = \int_0^T G \left(\lambda(t)|a_0 = 0,1, x_1, x_2 \dots\right) dt \quad (3)$$

Denote $(\Lambda|a_0 = 0, x_1, x_2 \dots)$ as $\Lambda_{0,1}$. Similarly Λ_1 can be defined. Then, the number of electrons C generated due to the random photodetection process is Poisson distributed:

$$p(c|\Lambda_{0,1}) = \frac{\Lambda_{0,1}^c \exp(-\Lambda_{0,1})}{c!} \quad (4)$$

Then the conditional moment generating function (MGF) $M_C(s|a_0 = 0,1)$ is given by:

$$M_C(s|a_0 = 0,1) = \sum \left[\sum_0^{\infty} p(c|\Lambda_{0,1}) e^{sc} \right] p(x_1, x_2 \dots x_n) \quad (5)$$

A Gaussian process can model the moment generating function of the zero-mean thermal noise $MT(s)$:

$$M_T(s) = \exp\left(\frac{\sigma^2 s^2}{2}\right) \quad (6)$$

The variance of electrons σ^2 is given by:

$$\sigma^2 = N_{th} \int_{-\infty}^{\infty} |H_R(f)|^2 df \quad (7)$$

In the case of an ideal integrator with period T_b ,

$$\sigma^2 = N_{th} T_b \quad (8)$$

The resulting MGF $M_Z(s)$ for the decision device is given by the product of the two mgf's.

$$M_Z(s|a_0 = 0,1) = M_C(s|a_0 = 0,1) \times M_T(s) \quad (9)$$

The bit error rate can then be calculated using the saddlepoint approximation. For details of the saddlepoint approximation please see [14], [15]. In order to take into account the effect of the interfering crosstalk channel, the power has now to be conditioned to take into account the random variables affecting the electrical field in the interfering channel; and the random variables affecting the interaction between the channels.

These include variables such as the pattern of past bits in the interfering channels; optical phase mismatch; and the delay offset between the channels. The delay offset is the time difference between bit transitions in the interfering and data channels. The expression for the interfering field $E_{\text{interfering}}(t)$ is given by:

$$E_{\text{interfering}}(t) = B \cdot \sum_{j=-\infty}^{\infty} b_j g(t - \Delta\tau - jT_{b,\text{interfering}}) \quad (10)$$

where B is the amplitude of the field, b_j is either a '0' or a '1', and $g(t)$ is the normalized pulse shape used in the interfering channel and $\Delta\tau$ is the delay offset.

Then, Λ_0 and Λ_1 is modified to include conditioning on these new variables. The same calculations as detailed in equations (11) – (15) and the saddlepoint approximation can be carried out to determine the bit error rate with crosstalk degradation. This method has been shown to be extremely accurate in determining the BER with crosstalk degradation. 16

4. ARCHITECTURE USED IN SIMULATION

This study considers the crosstalk degradation for a single-hop in the OSCM router network of Figure 1, using the analysis of Section 3. Separate BB and SC signals are combined using the MUX demonstrated in [8], [9] and demultiplexed using the DMUX receiver demonstrated in 10. The BB is a 10 Gb/s NRZ signal and the SC is a 2.5 Gb/s NRZ signal. Figure 4 shows a complete diagram of the system.

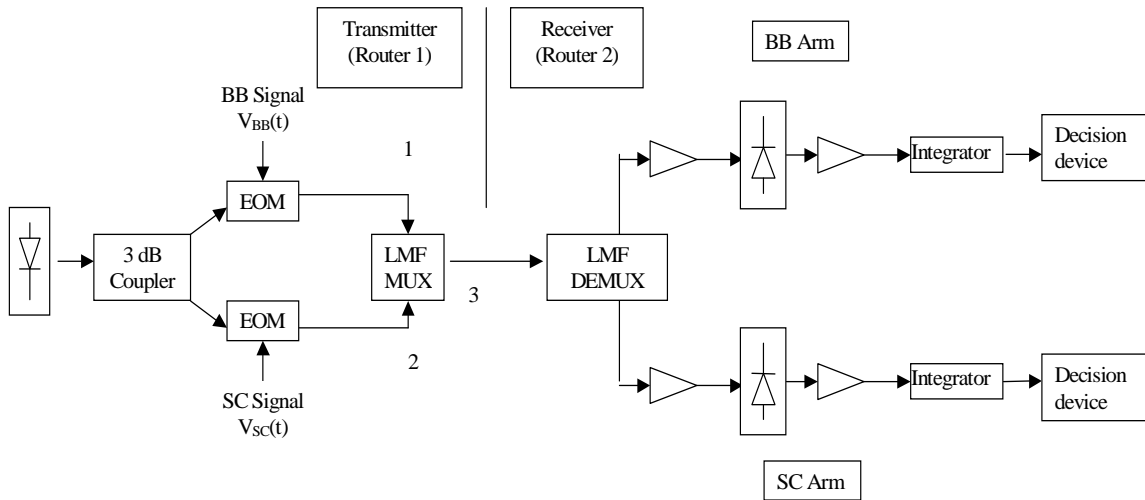


Figure 4: Architecture used in Simulation

4.1 The Transmitter

In the transmitter section of Figure 4, the laser signal is split between the BB and SC arms, and data is separately modulated on both the channels before combination of the two signals using the MUX. The typical linewidth of a semiconductor laser is approximately 2 MHz, [17], implying that the coherence time is 80 ns. Since this is long relative to the period during which the BB and SC signals influence the transient response of the filters, in this simulation the laser is modeled as a zero-linewidth laser, operating at 1550 nm. The intensity transfer functions of the modulators in the BB and SC arms have been obtained from measured data for an electro-optic modulator (EOM). It is given by:

$$P_{out}(t) = P_o \cos^2 \left[\frac{\pi(V(t) - V_{off})}{2V_\pi} \right] \quad (11)$$

where V_π is the half-wave voltage, V_{off} is the voltage needed for peak transmission. As in [12], for this simulation, V_π is 6.99 V, and $V_{off} = 1.21$ V. P_o is given by $P_{in}L$, where L is the insertion loss, and P_{in} is the input power.

In the BB arm, the electro-optic modulator is biased so as to allow maximum extinction ratio between a '0' and a '1'. The BB input voltage is assumed to be:

$$V_{BB}(t) = V_{bias, BB} + V_{1, BB} \cdot \sum_{k=-\infty}^{\infty} a_k h(t - kT_{b, BB}) \quad (12)$$

where a_k is a 1 or a 0, with equal probability. $T_{b, BB}$ is the bit period, and $h(t)$ is the pulse shape for an NRZ signal, given by:

$$h(t) = \begin{cases} 1, & 0 < t < T_{b, BB} \\ 0, & otherwise \end{cases} \quad (13)$$

In the case of the BB signal, in order to obtain as large an extinction ratio as possible, the optimum bias is at $(2n+1)V_\pi + V_{off}$, such that for a '0' symbol, no power is transmitted [18]. After modulation the BB signal is an on-off NRZ signal in the optical domain.

For the SC signal, the input voltage is given by:

$$V_{SC}(t) = V_{bias, SC} + V_{1, SC} \cdot \sum_{q=-\infty}^{\infty} b_q g(t - qT_{b, SC}) \quad (14)$$

where b_k is a 1 or a 0, with equal probability. $T_{b, SC}$ is the subcarrier bit period, and $g(t)$ is the pulse shape, given by:

$$g(t) = \begin{cases} \cos(\omega_{SC}t + \psi), & 0 < t < T_{b, SC} \\ 0, & otherwise \end{cases} \quad (15)$$

ψ is the electrical phase uncertainty of the subcarrier, and ω_{SC} is the electrical subcarrier angular frequency, where $\omega_{SC} = 2\pi f_{SC}$. Thus, the subcarrier signal is generated using the same laser as the baseband signal. As in 9, the f_{SC} is 16.66 GHz. It is assumed that both the BB and SC signals are linearly polarized at 45°. The polarization state used for the simulation is not important, as the LMF is polarization independent [10].

The subcarrier signal is an amplitude modulated (AM) signal. For the subcarrier signal, the optimal bias is at $V_{off} + (2n-1/2)V_\pi$ [18]. Then for a '1', the envelope $E_{SC}(t)$ takes the form:

$$\begin{aligned}
E_{SC}(t) &= \sqrt{P_o} \cos \left[\left(\frac{\pi V}{2V_\pi} \right) \sin \left(\omega_s t + \psi + \frac{\pi}{2} \right) - \frac{\pi}{4} \right] \\
&= \sqrt{\frac{P_o}{2}} \cos \left[\left(\frac{\pi V}{2V_\pi} \right) \sin \left(\omega_s t + \psi + \frac{\pi}{2} \right) \right] + \sqrt{\frac{P_o}{2}} \sin \left[\left(\frac{\pi V}{2V_\pi} \right) \sin \left(\omega_s t + \psi + \frac{\pi}{2} \right) \right] \\
&= \sqrt{\frac{P_o}{2}} \left[J_0(\beta) + 2 \sum_{n=1}^{\infty} J_{2n-1}(\beta) \sin \left[(2n-1) \left(\omega_s t + \psi + \frac{\pi}{2} \right) \right] \right] \\
&\quad \left[+ 2 \sum_{n=1}^{\infty} J_{2n}(\beta) \cos \left[2n \left(\omega_s t + \psi + \frac{\pi}{2} \right) \right] \right]
\end{aligned} \tag{16}$$

where $J_n(x)$ is the Bessel function of the first kind, and β is defined as:

$$\beta = \frac{\pi V}{2V_\pi} \tag{17}$$

Thus components exist at all harmonics of the SC frequency f_{SC} . The power contained in a '1' is given by:

$$\begin{aligned}
P_{1,SC} &= \frac{P_o}{2} \sum_{n=-\infty}^{\infty} J_n^2(\beta) \\
&= \frac{P_o}{2}
\end{aligned} \tag{18}$$

For a '0', the power contained is given by:

$$\begin{aligned}
P_{0,SC} &= P_o \cos^2 \left(\frac{\pi}{4} \right) \\
&= \frac{P_o}{2}
\end{aligned} \tag{19}$$

It is useful to define the optical modulation index μ for the amplitude-modulated subcarrier signal. Applying the general definition of the modulation index from [19], μ is defined as:

$$\mu = \frac{E_{SC,max} - E_{SC,min}}{E_{SC,max} + E_{SC,min}} \tag{20}$$

With the chosen biasing arrangement, $E_{SC,max}$ and $E_{SC,min}$ are:

$$\begin{aligned}
E_{SC,max} &= \sqrt{\frac{P_o}{2}} [\cos(\beta) + \sin(\beta)] \\
E_{SC,min} &= \sqrt{\frac{P_o}{2}} [\cos(\beta) - \sin(\beta)]
\end{aligned}$$

(21)

Then, μ is given by:

$$\mu = \tan(\beta)$$

(22)

For small β , $\mu = \beta$. The modulation indices used in the simulation are 0.10, 0.20, 0.30, 0.40, 0.50, 0.60, 0.80 and 1.00. The operation of the LMF MUX has been described in detail in [9]. The experimental and simulation results for the power transfer functions were shown to agree closely there.

4.2 The Receiver

In the receiver section of Figure 4, the DMUX separates the BB from the SC signal. The two separate signals are then optically amplified in their respective arms before detection. After this, in each signal the data is electrically amplified, shaped using an ideal integrator filter, and then sampled at a given instant using an ideal sampler.

The LMF DMUX works the same way as the LMF MUX. The transfer function for the DMUX input-SC arm is the same as the transfer function for the SC input-MUX output; similarly for the BB signal. The optical preamplifier is assumed noiseless for the purposes of this simulation, so as to not overly complicate the analysis and help identify the main power penalties. The photodetector is assumed to have a quantum efficiency of 1.

Referring to Figure 4, the thermal noise in the electrical amplifier in the receiver is adjusted so as to provide a receiver sensitivity for an optically preamplified receiver of -32 dBm for a bit error rate of 10^{-9} following the approach of [14]. The optimal sampling instant obtained by simulation for the BB signal sampler is 30 ps after the bit transition. For the SC signal sampler it is 60 ps.

5. APPLICATION OF NOVEL TRANSIENT ANALYSIS APPROACH TO SIMULATION ARCHITECTURE

5.1 The ISI Case

This calculation has been detailed in Section 3. The degradation solely due to the ISI in the BB and SC is calculated, conditioning over different combinations of past bits. For the BB case, it is assumed that because the optimal sampling instant is 30 ps after the bit transition, only bits a_{-1} , a_0 and a_1 are considered in the ISI calculation. The mean number of electrons $\lambda_{BB}(t)$ according to

(2) is given by:

$$\left(\lambda_{BB}(t) \middle| a_0 = 0,1, a_1, a_{-1}\right) = \frac{\eta}{h\nu} \left| \left(E_{BB}(t) \middle| a_0 = 0,1, a_1, a_{-1}\right) \right|^2$$

(23)

The calculation then follows the remaining steps of Section 3. For the SC case, the optimal sampling instant is 60 ps after the transition. Hence similarly only bits b_{-1} , b_0 , and b_1 are considered. The electrical phase uncertainty ψ of the modulating signal must also be considered, and is assumed to be uniform on $[-\pi, \pi]$. Thus following

(2), the mean number of electrons $\lambda_{SC}(t)$ can then be conditioned on these variables, and can be expressed as:

$$\left(\lambda_{SC}(t) \middle| b_0 = 0,1, b_1, b_{-1}, \psi\right) = \frac{\eta}{h\nu} \left| \left(E_{SC}(t) \middle| b_0 = 0,1, b_1, b_{-1}, \psi\right) \right|^2$$

(24)

5.2 The Crosstalk Case

The BER is then calculated to incorporate the crosstalk degradation using the approach of Section 3. For the interaction between the two channels, two random variables are considered: optical phase mismatch and delay offset arising due to random misalignment between the bit streams. Optical phase mismatch occurs when there is a phase difference between the optical path lengths in the BB and SC channels. The random bit stream misalignment occurs before multiplexing, and arises due to either: path difference after modulation between the modulated BB and SC signals entering the MUX; and/or delay between the times of arrival of the bit streams to the BB and to the SC modulator.

For this study, the optical phase mismatch is assumed to be 180° between the baseband and subcarrier, which is the worst case scenario. The delay offset $\Delta\tau$ is assumed to be between $[0, T_{b,SC}]$ in the case when the BB is the data channel and the SC is the interfering channel. The ISI effect is limited to b_{-2} instead of b_{-1} as previously. This allows for the case where the SC bit transition occurs in the middle of the baseband bit slot so that the baseband bit slot spans two bits in the subcarrier.

For the SC case, the delay offset is assumed uniform on $[0, T_{b,BB}]$. The calculation is complicated, as for each subcarrier bit, there is either N or $N+1$ interfering baseband bits, depending on the timing of the bit transition. N is defined as $\lfloor \text{Baseband Bit Rate} / \text{Subcarrier Bit Rate} \rfloor$. For a 10 Gb/s baseband and 2.5 Gb/s subcarrier, $N = 4$. Also the previous baseband bit must be considered, meaning 2^5 combinations of bits must be considered for each subcarrier bit.

6. RESULTS

Figure 5 shows the BER for the BB signal for the back-to-back; the signal after passing through the LMF; and the BB signal with crosstalk corruption. Most of the degradation is due to ISI after passing through the LMF. The power penalty between the back to back BER curve and the BER curves obtained after the passage of the BB signal through the LMF is 1.6 dB. The BB signal is insensitive to SC interference, as a further 0.2 dB penalty is incurred due to interference from the SC signal.

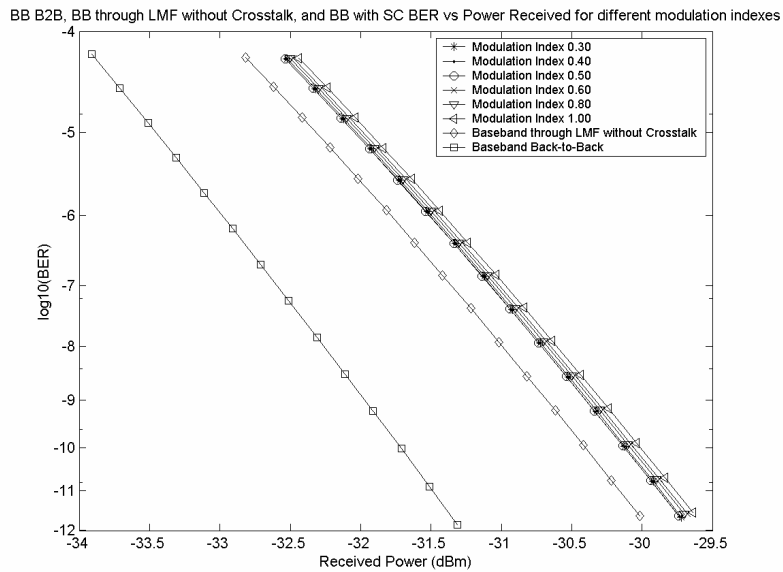


Figure 5: BER for the BB Signal

Figure 6 shows the variation in BER with modulation index for the SC signal after passing through the LMF. The receiver sensitivity does not vary much with the modulation index. For all the values of modulation index used in the simulation, the receiver sensitivity is between -34.4 and -34.6 dBm.

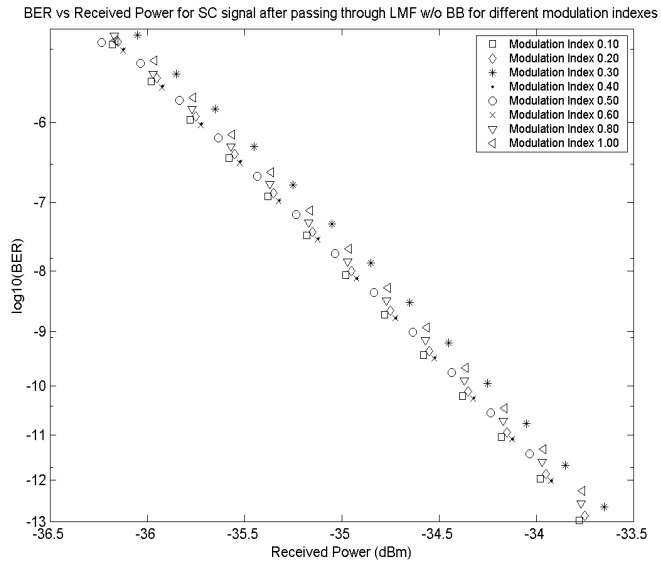


Figure 6: BER for the SC Signal without the BB for different values of modulation index

Figure 7 shows the variation in BER with modulation index for the SC signal when it is combined with the BB signal. The power penalty due to interference from the BB signal decreases with modulation index.

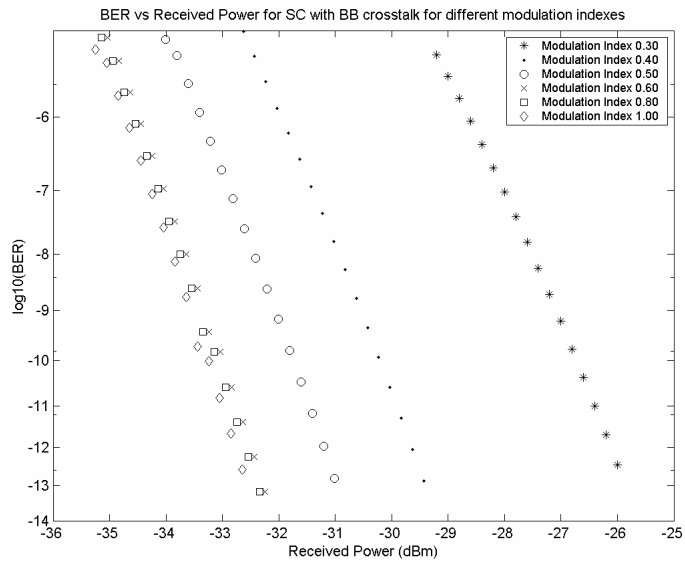


Figure 7: BER for the SC signal with BB crosstalk

For the 0.10 and 0.20 modulation indexes, a BER of 10^{-9} cannot be achieved. This is because the probability density function (pdf) for the electron counts for a '0' received and a '1' received overlap, implying that under BB interference, a BER floor is formed. For higher values of μ the pdfs are non-overlapping, implying that BER can be increased with received power.

Figure 8 shows the receiver sensitivity plotted against μ . The highest penalty obtained is 7.3 dB for a modulation index of 0.30, and 0.9 dB for a modulation index of 1.00. This increased tolerance of the SC signal to BB signal interference is due to more power in the sidebands. Increasing μ leads to reduction of signal suppression and crosstalk degradation. But it requires a higher RF power. For example, to move from a μ of 0.30 to a μ of 0.60 requires an extra 5 dB of RF power.

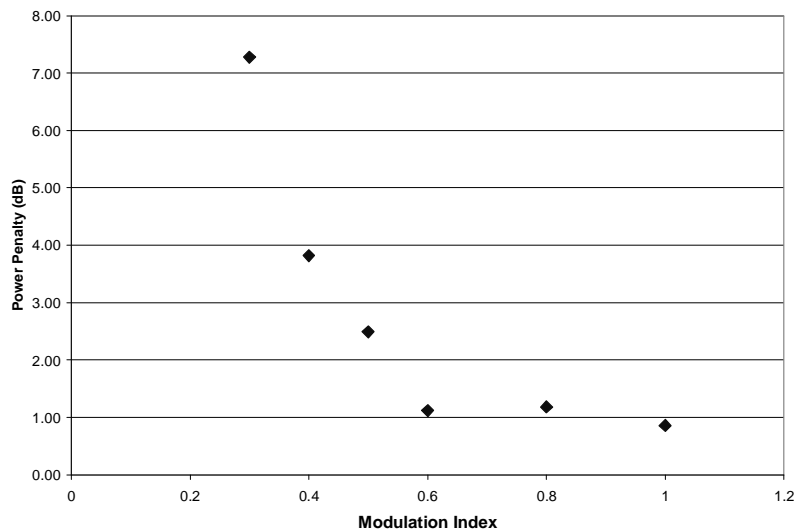


Figure 8: Power penalty for SC Crosstalk vs modulation index

7. CONCLUSION

The calculation of ISI and crosstalk degradation for a single-hop in a network controlled by OSCM routers has been carried out. The BB signal suffers little degradation due to the presence of the SC signal. The degradation due to crosstalk in the SC signal is sensitive to modulation index, and ranges from 0.90 to 7.30 dB.

REFERENCES

1. R. Gaudino, M. Len, G. Desa, M. Shell and D. J. Blumenthal, "MOSAIC: A multiwavelength optical subcarrier multiplexed controlled network," *IEEE J Select Areas Commun.* pp. 1270-1285 vol 16 no 7 Sept 1998
2. E. Park, A. E. Willner, "Network demonstration of self-routing wavelength packets using an all-optical wavelength shifter and QPSK subcarrier routing control" pp. 114-115 *OFC '96*, vol 2
3. T. E. Dimmick, G. Rossi and D. J. Blumenthal, "Optical dispersion monitoring technique using double sideband subcarriers", *IEEE Phot Tech Lett* pp. 900 – 02 vol 1 no 7 July 2000
4. G. Rossi, T. E. Dimmick and D. J. Blumenthal, "Optical performance monitoring in reconfigurable WDM optical networks using subcarrier multiplexing," *IEEE J Lightwave Tech* pp. 1639-48 vol 18 no 12 Dec 2000
5. D. J. Blumenthal, A. Carena, L. Rau, V. Curri and S. Humphries, "All-Optical Label Swapping with Wavelength Conversion for WDM-IP Networks with Subcarrier Multiplexed Addressing," *IEEE Phot Tech Lett* pp. 1497-1499 vol 11 no 11 Nov 1999
6. H. J. Lee, S. J. B. Yoo, V. K. Tsui and S. K. H. Fong, "A Simple All-Optical Label Detection and Swapping Technique Incorporating a Fiber Bragg Grating Filter," *IEEE Phot Tech Lett* pp. 635-637 vol 13 no 6 June 2001
7. Y. M. Lin, W. I. Way, and G. K. Chang, "A Novel Optical Label Swapping Technique Using Erasable Optical Single-Sideband Subcarrier Label," *IEEE Phot Tech Lett* pp. 1688-1690 vol 12 no 8 Aug 2000

8. T. E. Dimmick, R. Doshi, R. Rajaduray, G. Rossi, B.-E. Olsson, D. J. Blumenthal, "Optically Multiplexed Transmitter for Hybrid Baseband and Subcarrier Multiplexed Signals," *ECOC '00*, Session 6.2 paper 5
9. R. Rajaduray, R. Doshi and D. J. Blumenthal, "Optical Multiplexing for Subcarrier Multiplexed Systems with Carrier Suppression for Subcarrier Signals," *to be submitted to IEEE J. Lightwave Tech*
10. G. Rossi, O. Jerphagnon, B. -E. Olsson, D. J. Blumenthal, "Optical SCM data extraction using a fiber-loop mirror for WDM network systems," *IEEE Phot. Tech. Letters*, pp. 897-9 vol 12 no 7 July 2000
11. J. Marti, J. Capmany and H. Mangharam, "Crosstalk analysis in optically prefiltered subcarrier multiplexed systems" *IEE Elect Lett* pp. 2054-55 vol 29 no 23 11th November 1993
12. P. Chamorro-Posada, F. J. Fraile-Pealez, R. Gomez-Alcala and D. Pastor, "Performance Analysis of Optical Prefiltering-SCM Systems by Accurate Spectral Techniques" *IEEE Phot Tech Lett* pp. 85-87 vol 12 no 1 Jan 2000
13. J. Marti and J. Capmany, "Modeling Optically Prefiltered AM Subcarrier Multiplexed Systems", *IEEE Trans on Micro Theory and Tech* pp. 2249-56 vol 43 no 9 Sep 1995
14. S. L. Danielsen, B. Mikkelsen, T. Durhuus, C. Joergensen, K. E. Stubkjaer, "Detailed Noise Statistics for an Optically Preamplified Direct Detection Receiver", *IEEE J. Lightwave Tech* pp. 977-82 vol 13 no 5 May 1995
15. G. Einarsson, *Principles of Lightwave Communications*, Chichester: Wiley, 1996
16. I. T. Monroy, E. Tangdionga and H. de Waardt, "On the Distribution and Performance Implications of Filtered Interferometric Crosstalk in Optical WDM Networks" , *IEEE J Lightwave Tech* pp. 989-97 vol 17 no 6
17. http://www.agere.com/long_haul_backbone/docs/DS00166-1.pdf
18. R. Gaudino and D. J. Blumenthal, "A novel transmitter architecture for combined baseband data and subcarrier-multiplexed control links using differential Mach-Zehnder external modulators," *IEEE Phot Tech Letters*, pp. 1397 – 99 vol 9 no 10 Oct 1997
19. S. Haykin *Communication Systems* 3rd ed New York ,Wiley 1994